

Magic Angle Chaotic Precession

Bernd Binder (CHAOS2008 conference Greece/Grete/Chania, 13.6. 2008)

Quanics, Salem, Germany,
Email: binder@quanics.com

Abstract: This paper explores the properties of a precessing rotor or a coupled system of precessing rotors (gyroscopes), where a special chaotic behavior in the precession angle can be found if the change of rotor angular velocity is linearly coupled by (an)holonomy to the precession angular velocity and angle. The linear coupling provides for rolling cone paths and allows spinning up and controlling the rotor simply by forcing precession at special quantum magic precession angles. This linear relation models a recurrent chaotic holonomy, where precession as the effect of holonomy is also a cause of holonomy linearly related to the rotator spin. The geometric phase induced by the curved path of the rotor or external curvature and part of the coupling increases with precession angle. This leads to bifurcations in coupling strength resulting in chaotic precession. As an alternative to the $SO(3)$ matrix or quaternion representation the treatment of the three coupled rotations is here based on Euler's dynamical equations. First, the classical Magic Angle Precession (MAP) dynamics is realized by a geometric or mechanical condition (type I, transcendental solutions), where it can be experimentally demonstrated how MAP can "slave" angular degrees of freedom allowing the external control of high-frequent spin by slow oscillations. MAP can be found in a commercial fitness device and conceptually approached via Chua's electric circuit. Second, the quantum-gravitational MAP (type II, rational solutions) with discrete precession angles is analyzed on a deeper level requiring intrinsic curvature/relativistic effects adjusting holonomy to topological numbers. Third, a macroscopic network of MAP elements is presented as a discrete-time recurrent neural network synchronizing to one common MAP I/II dynamics under special pairing and symmetry conditions (type III). In all three cases MAP can be treated as a time-discrete chaotic system with singularities given by the cosine map with several possible links to interesting applications on all scales.

Keywords: Chaotic precession, Spin-orbit coupling, Gyroscope, Magic Angle, Euler's Equations, $SO(3)$, Bifurcation, neural net, Chua, Berry, Hannay.

Introduction

Rotated spin systems like gyroscopes, precessing stars, rotating solids, superconductors, electromagnetic particles, or others are very interesting from many different points of view. Adding a few extra coupling or damping terms, which is typical for a real system, can lead to chaotic precession (like a dissipation induced instability or bifurcation [1]), where it is rather expensive to actively control chaotic motion to obtain the sufficient stability conditions at the equilibrium points even for relatively simple gyroscope systems [2]. Regarding this challenge and the broad spectrum of possible physical applications we focus on special conditions supporting fast auto-tuning and self-stabilization capabilities. In [3], [4], and [5] we have already identified a rather basic chaotic mechanism given by the cosine map, where the

precession angle of rotated rotors can iterate towards an optimum. This situation arises if the precession angle induced by an external or internal coupling becomes linearly related by a connection or (an)holonomy to the spin frequency shift of precession. Recently we were able to show [5] that the basic mechanism can be illustrated and experimented with well known commercial gyroscopes useful as a hand fitness device [6], but there is almost no published literature about its chaotic precession properties [7]. In this paper

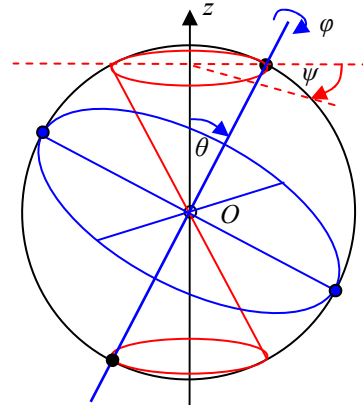


Figure 1. The rotor (blue), Euler angles, and precession cone (red).

we will work out the dynamical equations of MAP. Comparing the classical transcendental recursion (type I) to the rational recursion (type II), there is some number theoretical evidence that type II requires relativistic degrees of freedom to realize quantum boundary conditions like quantum spin and precession numbers. Introducing the MAP spin network (type III) and some symmetry conditions the network can behave as one MAP element. The emerging differential or difference equations of precession provide for attracting and repelling “charge” singularities including broken symmetry, which has similarities to Chua’s Circuit. This helps to evaluate both, the classical and quantum-gravitational context of MAP.

1. Transcendental Spin-Orbit Recursion (MAP Type I)

1.1. Kinematics, frequencies, and frequency shift in flat space

As an alternative to the $SO(3)$ matrix [4] or quaternion representation, we start with Euler’s dynamical equations [8],[9] based on angular relations. In Euler’s dynamical equations the angular velocity vector is expressed by three Euler angles describing the motion of the advancing frame with respect to the inertial frame. With mass points rotating and precessing on the sphere in flat space (which is a classical connection) the three Euler angles are, see fig.1:

1. θ , first Euler angle describing the precession tilt angle,
2. φ , second Euler angle describing the spin of the rotor axis,
3. ψ , third Euler angle describing the precession of the axis.

In Cartesian coordinates the rotor will precess around the z -axis. Assume that the rotor axis of a spherical rotating rotor precesses at frequency $\omega_\psi = d\psi/dt$. The temporal change of precession tilt given by $\omega_\theta = d\theta/dt$ will be called nutation. As a characteristics of precession the rotor rotating at frequency $\omega_\varphi = d\varphi/dt$ will experience a frequency shift ω_Δ , which is part of the invariant component ω_r given by the 3rd dynamical equation

$$\omega_r = \omega_\varphi + \omega_\Delta = \omega_\varphi + \omega_\psi \cos \theta, \quad \omega_\Delta = \omega_\psi \cos \theta, \quad (1)$$

(see [9] with notation $\omega_r = r$, $\omega_{p,q}^2 = p^2 + q^2$). With eq.(1) and according to [9] the kinetic energy T of the spherical symmetry is given by

$$T = \frac{1}{2} \omega_{p,q}^2 + \frac{1}{2} \omega_r^2 = \frac{1}{2} (\omega_\theta^2 + \omega_\psi^2 + \omega_\phi^2) + \omega_\Delta (\omega_r - \omega_\Delta). \quad (2)$$

From one Euler's equation, the other two follow by symmetry [9], where

$$\omega_{p,q}^2 = \omega_\theta^2 + \omega_\psi^2 \sin^2 \theta \quad \text{and} \quad \omega_\theta^2 + \omega_\psi^2 = \omega_{p,q}^2 + \omega_\Delta^2. \quad (3)$$

1.2. Geometric phase from (an)holonomy

Geometric phases naturally arise in the dynamics of coupled rigid bodies [10], [11], [1] (i.e. rolling on each other) or in curved space-time. Therefore, we will introduce $\bar{\theta}$ as a geometric phase or the Hannay anholonomy of the $U(1)$ bundle along the curve, where the 'parallel transported' spin vector (rotor axis) will come back after every loop or cyclic evolution with missing (i.e. spherical) or extra (i.e. hyperbolic) rotations equal to the curvature enclosed by the path

(compare to the Gauss–Bonnet Theorem), [1], [11]. Generally, to measure the corresponding topological winding numbers within a given period T we can count the corresponding number of extra or missing loops j out of N as the holonomic (spin) current, which can be assigned to a topological sector (surface area). For gyroscopic motion on the unit sphere S^2 with unit Gauss curvature there are j spin loops out of N transferred from rotational to precessional motion as the spin current driven by precession is given by the spherical area Ω the precession axis sweeps

$$\Omega = T \omega_{\bar{\theta}} = 2\pi \frac{\omega_{\bar{\theta}}}{\omega_\psi} = 2\pi (1 - \cos \theta) = 2\bar{\theta} = \frac{2\pi j}{N}, \quad T = \frac{2\pi}{\omega_\psi}. \quad (4)$$

So j and N are numbers characterizing the phase/frequency shift or current induced by external accelerations or equivalently relativistic effects (by motion or curvature), which can be treated as Chern-Simons type gauge fields. Regarding a higher-dimensional holonomy (Berry-Hannay on S^2) we expect that precession will also acquire a geometric part in addition to the dynamical part. This is the core assumption leading to a *recurrent chaotic holonomy*, where the cause of holonomy is also a generator of holonomy. Characterizing the dynamical part of precession by a number M , the 3rd dynamical invariant ω_r is M -times the precession frequency

$$\omega_r = \omega_\psi M. \quad (5)$$

The special case $M = 1$ corresponds to $\omega_r = \omega_\psi$, $|\theta| = \pi/2$, and $j = 1$, with $\omega_r = N\omega_1$ and $\omega_{\bar{\theta}} = \omega_1 = \omega_\phi$, see figs.1 and 2.

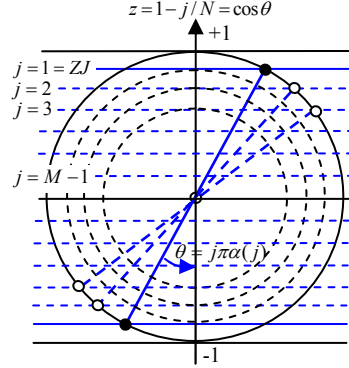


Figure 2. Geometric phases and precession with $|j/N| > 0$. Here $M=7$.

1.3. The coupling parameter α

According to eqs.(1)-(5) the dynamical phase Δ or total phase minus geometric phase can be found in the z -axis with $z = \cos \theta$ from the tilt/precession angle θ in terms of j and N , see fig.2. This dynamical part is given by the transcendental number (the rational case will be MAP type II)

$$\frac{\omega_\Delta}{\omega_\psi} = \cos \theta = \frac{N-j}{N}, \quad 0 < j < N, \quad \Delta = \pi(N-j), \quad \omega_\Delta = \frac{d\Delta}{dt}. \quad (6)$$

According to eqs.(4) and (6) the coupling and corresponding frequency shift can be interpreted as a geometric phase changing the precession frequency, where the product $\omega_\Delta \omega_{\bar{\theta}}$ is linearly related to the nutation frequency ω_θ

$$\omega_\Delta = \omega_\psi - \omega_{\bar{\theta}} = \omega_r - \omega_\phi, \quad \omega_\theta \omega_\psi = \omega_\Delta \omega_{\bar{\theta}}. \quad (7)$$

The coupling parameter describing the shift and dynamical phase evolution within one precession loop can be defined according to eqs.(4-7) by

$$\alpha = \frac{\cos \theta}{M} = \frac{\omega_\Delta}{\omega_r} = \frac{\omega_\psi - \omega_{\bar{\theta}}}{\omega_r} = \frac{1}{M} - \frac{\omega_{\bar{\theta}}}{\omega_r} = \frac{N-j}{NM}. \quad (8)$$

Eq.(8) can characterize the fine structure of spin-orbit coupling [3]. With eq.(2) the coupling constant $|\alpha| > 0$ leads to a shift $|\omega_\Delta| > 0$, $\alpha = 0$ corresponds either to $\omega_\psi = 0$ or $|\theta| = \pi/2$, see the red curve in fig.3. Assuming positive frequencies and $\omega_1 = \omega_{\bar{\theta}} (j=1)$ we get with eqs.(1)-(8) $\omega_r > \omega_\phi > \omega_\psi > \omega_\Delta > \omega_{\bar{\theta}} > \omega_\theta$, where

$$\omega_1 = \frac{\omega_r}{MN} = \frac{\omega_\phi}{N(M-1)+j} = \frac{\omega_\psi}{N} = \frac{\omega_\Delta}{N-j} = \frac{\omega_{\bar{\theta}}}{j} = \frac{N\omega_\theta}{j(N-j)}. \quad (9)$$

1.4. Recurrent holonomy as the geometric feedback condition

We assume that the holonomy on the sphere is isotropically "contracting" not only the azimuthal ($\psi, 0 \dots 2\pi$) but also the zenithal range ($\theta, 0 \dots \pi$) down by a rational factor $(N-j)/N$. Now both, the cone apex and dynamical phase Δ for one precession cycle become similarly contracted according to eq.(7), where the evolution for one loop $T \sim dt/d\psi$ (assuming ψ, Δ , and the geometric phase evolve proportional to the precession frequency) should provide for a precession angle proportional to the product of dynamical and geometric phase leading to $\theta \sim j\Delta$ according to eq.(7). As a criterion for precessional coupling, the precession angle subject to dissipation will nutate according to eq.(7). The corresponding Jacobian flow and response within T (one precession period) will be given by a minimum action which is the holonomy corresponding to one rotator loop, where the resulting coupling is proportional to precession

$$-\omega_1 \frac{\theta}{\pi} = \frac{1}{M} \frac{d\theta}{dt} = \alpha \omega_{\bar{\theta}}, \quad \theta = \pi j \alpha. \quad (10)$$

Since the geometric phase $\bar{\theta}_t$ is evaluated within one discrete precession loop period, the precession angle for a new precession period T_{t+1} at time $t+1$ is

determined by the dynamics and precession angle of the previous period T_t at time t providing with eq.(10) for a time-discrete coupling $\alpha_t(\theta_t)$ and angle

$$\theta_{t+1} = \pi j_t \alpha_t(\theta_t) = \frac{\pi}{M} \frac{j_t}{N_t} (N_t - j_t) = \pi j_t \frac{\omega_{\Delta,t}}{\omega_{r,t}}. \quad (11)$$

Because of the recursive relation between geometric phase contribution $\bar{\theta}_t$ and the precession angle in eq.(11) we can expect chaotic precession. With a dimensionless z -variable according to fig.2 and the z -Phase $\tilde{\theta}_t$

$$z_{t+1} \propto \theta_t(z_t), \quad z_t = 1 - \frac{j_t}{N_t} = 1 - \frac{\bar{\theta}_t}{\pi} = \frac{\tilde{\theta}_t}{\pi}, \quad (12)$$

the number j of geometric extra loops in eq.(11) become in the stable case the fixed points $j = N(1 - M\alpha)$ of a logistic map, whereas $\tilde{\theta}_{t+1}$ or the precession angle can be iteratively computed from a time-discrete cosine chaotic map

$$\begin{aligned} \tilde{\theta}_{t+1} &= \pi \cos \tilde{\theta}_t, \\ \theta_{t+1} M &= j \pi \cos \theta_t, \end{aligned} \quad (13)$$

showing the Feigenbaum scaling property with bifurcations (see figs.3,5). With the precession angle linearly related to the spinning phase/ frequency offset induced by precession we have the MAP feedback situation recursively adjusting or auto-tuning the precession angle and frequency to the external acceleration source eventually leading to coupling anomalies [14]. Since the cosine map eq.(13) has a set of quadratic extrema, the scenario of transition to chaos can be characterized by period-doublings. The first bifurcation is the second contact or intersection (singularity) of the nonlinear $\cos \theta$ and the linear coupling term proportional to θ , see fig.3, the tangent to the cosine function (slope is given by the sine function) at $\theta \tan \theta = \pm 1$ with $\theta = 0.5\pi \cdot 0.8603336\dots$ and $j/M \sim 0.839801\dots$

1.5. Approaching the dynamics of MAP with Chua's Circuit

To model the chaotic precession / nutation dynamics in eqs.(10)-(13) we can refer to a well known and rather simple system of coupled differential equations, where the angular/phase space occupation density and flow of the attractor can be simulated and visualized, see fig.4 (the time discrete simulation uses the difference equation version)

$$\begin{aligned} dz &= \omega_\psi M (y - z) dt + \omega_\psi f(y - z) dt, \\ dy &= \omega_\psi x dt - \omega_\psi M (y - z) dt, \\ dx &= -\omega_\psi y dt, \end{aligned} \quad (14)$$

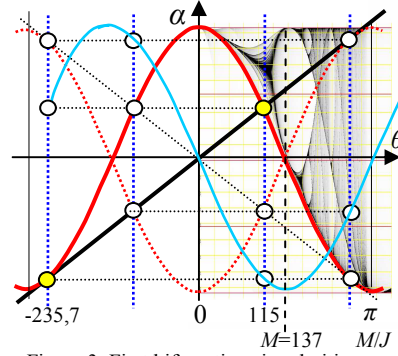


Figure 3. First bifurcation singularities (yellow) at $j/M \sim 0.839801\dots$ from $-\theta \tan \theta = 1, \theta = \pm 0.8603336\dots$

$$\text{with } \pi x = \tilde{\theta}, \quad \pi j \alpha = \theta = j(y-z), \quad f(y-z) = \pm \pi \cos[j(y-z)].$$

This is a form of Chua's electronic circuit, a well known and real-world example showing chaotic dynamics [12]. MAP can be approached and illustrated if we take the precession angle as the voltage term (showing Coulomb type "charge" and dipole effects) and the rotor spin as the electric current (showing magnetic monopole

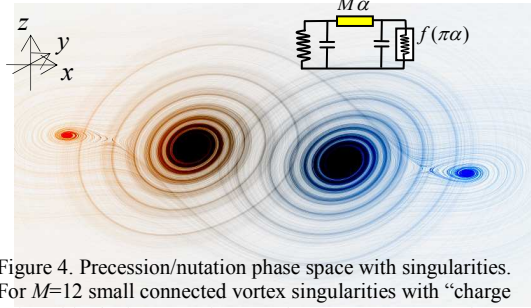


Figure 4. Precession/nutation phase space with singularities. For $M=12$ small connected vortex singularities with "charge pairs" (blue/red) appear for $j>10$, here $j=12$, see (14). The yellow conductive/coupling term provides for dissipation.

[8] and dipole effects). Both systems have 3 degrees of freedom (two voltage y, z , one current x) and 3 energy storage elements (two capacitors and one inductivity as the rotor angular momentum setting the timescale $\omega_r = \omega_\psi M$). In both cases a linear oscillator (precession in MAP) is coupled to a nonlinear element (anholonomy in MAP). The nonlinear element $f(\theta)$ responsible for chaos and bifurcation is driven by precession $\theta = j(y-z)$, where the geometric spin current is driven by a precession or corresponding scalar gauge potential gradient $(y-z)$ delivered through the spin "conductivity" of a monopole with strength M . Both systems show vortex singularities at points where the linear coupling current equals the nonlinear current. Bifurcation starts according to fig.3 for $|j/M| \approx 0.84$, where a small oppositely charged vortex singularity (see red point in fig.5) shows up at the end of the smeared out bifurcation zone near $|j/M| \geq 0.95$. With eqs.(10)-(13) we get near the vortex singularities ($dx/dt = dy/dt = 0$) a spiraling in plane $j\theta = M\theta$, the MAP condition can be found in eq.(14) from $dz/dt = d\tilde{\theta}/dt = 0$, nutation can be assigned to $d\theta/dt \neq 0$.

1.6. Powerball example

Based on this analysis it was recently proposed [5] that the MAP type I conditions are present in the "Powerball" system [6], [7]. The function of this device is based on a mechanical gear-type coupling between precession and spin frequency, see eq.(11). The rolling axis diameter at the end of the rotor shaft (#28 in [6]) is usually about 2 mm, the diameter of the groove (#24) or bearing ring element (#30) about 60 mm providing for $N \sim 30 = 60\text{mm}/2\text{mm}$ that counts how often the spin axis has to roll in the circular bearing to turn its axis by 360° with precession angle $\theta = \pi/2$, where $\omega_\Delta = \omega_\psi$. A wobbling by the hand introduces (an)holonomy and a shift by $\omega_{\tilde{\theta}}$, see eqs.(6)-(10). The MAP angle is given by $\theta = \arccos[(N-j)/N]$, see fig.2, a Powerball with $N \sim 30$, $M \sim 12$ and $j = 1$ has $\theta(j=1) \sim 15^\circ$, bifurcation starts near $j=JZ \sim 10$ or 75° .

2. Polynomial Quantum-Gravitational Connection (Type II)

Type I provides according to eq.(13) transcendental solutions, but curvature (by relativity or external accelerations) can support periodicity with rational or polynomial solutions which look like closed loop rolling cone paths. Under the Lorentz rotation group $SO(3)$ rolling cone paths can describe anholonomy and precession (see e.g. [1],[3],[4],[11]) while providing for special periodicity conditions. In this case we get curves of constant precession

(Darboux) in the Frenet description from the periodicity condition in the $SO(3)$ rotation matrix representation in [4], characterizing the cone rotation by $\cos(2\pi N \cos \theta) = \cos[2\pi(N-j)] = 1$ related to the cone geometry with $N \in [1, 2, \dots] > j \in [\frac{1}{2}, 1, \frac{3}{2}, \dots]$ in a single-valued monochromatic loop.

2.1. Tschebyscheff polynomials of the first kind

With integral N, M, j we get periodicity and monochromatic precession, where eq.(11) becomes a closed loop current condition

$$\cos \theta = \cos(n\theta), \quad n = MN / j = \Delta / \theta. \quad (15)$$

Eq.(15) provides for a finite order Tschebyscheff polynomial solution $T_n(x)$

$$T_n(x) = \cos[n \arccos(x)], \quad \frac{d^2 T_n}{d\theta^2} + n^2 T_n = 0, \quad (16)$$

representing the MAP type II precession and geometric phase condition relating the first polynomial $T_1(x) = x$ and linear tilt/precession term as an amplitude/phase condition to a higher polynomial

$$T_n(x) = T_1(x) = x, \quad \text{where } T_{n+1}(x) = 2xT_n(x) - T_{n-1}(x). \quad (17)$$

The polynomial can be written as a sum or a product,

$$T_n(x) = \sum_{i=0}^{\text{Floor}(n/2)} \binom{n}{2i} x^{n-2i} (x^2-1)^i = 2^{n-1} \prod_{k=1}^n \left\{ x - \cos \left[\frac{(2k-1)\pi}{2n} \right] \right\}, \quad (18)$$

where the zeros are with eqs.(11) and (18) at $k = (N-j) + \frac{1}{2}$. Mapping the x -current to a 2-dimensional y, z -precession in circular coordinates (voltage projection in Chua's circuit we get a closed loop nutation pattern, see fig.6,

$$T_n(z = \cos \theta, y = \sin \theta) = \sum_{i=0}^{\text{Floor}(n/2)} \binom{n}{2i} z^{n-2i} (-y^2)^i. \quad (19)$$

With the phase advance proportional to frequency at a given time period, the Chebyshev relations above provide for a frequency filter connecting the 1- d current and the 2- d closed loop space-time holonomy and dynamics.

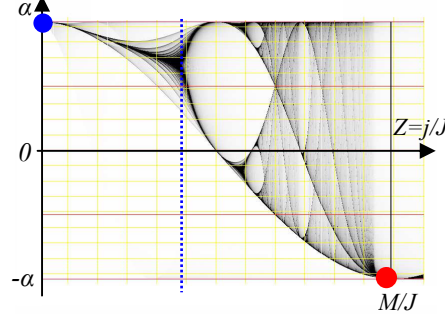


Figure 5. MAP bifurcation diagram [3],[4]. Smearing effects due to phase fluctuations. Points show the fig.4 vortex singularities.

2.2. MAP and Relativity

In General Relativity holonomy can be directly related to curvature, see

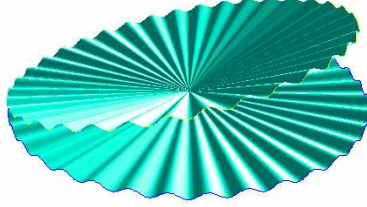


Figure 6. Closed modulated surfaces [4] by $2d$ Tschebyscheff polynomials in (19).

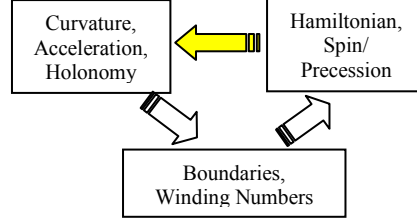


Figure 7. MAP recursive chaotic relation in space-time adjusting (an)holonomy.

i.e. [1],[10],[11],[13], where the precession induced by curvature and/or torsion angle is directly given by the coupling strength. W. de Sitter was the first who predicted geodetic precession in curved space-time [13], where the gyroscope will be carried by parallel transport along the path of free fall. Regarding MAP one could argue on a number theoretical level (15)-(19) that it is more economic to avoid transcendental and prefer rational or polynomial values based on (an)holonomy adjusted by recursion to periodicity, see fig.7. This would mean that there could be a natural preference for curved space-time and anholonomy supporting closed loop conditions on scales comparable to the self-coherence length, which is large in superconductors. MAP is expected to occur on all scales, see the table of candidates [14]. If we apply MAP as a coupling condition on the cosmic scale, the scale below the co-expanding unit scale appears to be contracting relative to the expanding unit scale, which is the inversion scale [15].

3. MAP Spin-Network Connection (Type III)

Precession dynamics including coupling according to eq.(14) can lead to synchronization in a network of coupled spins J_k . A “charged” discrete-time recurrent neural network can be found with a number Z of MAP elements connected by matrix coefficients ω_{ik} , if the resulting precession angle is the sum of all weighted components of the previous stage

$$\theta_{k,t+1} = \pi J_k \cos \left(\sum_{i=0}^{Z-1} \omega_{ik} \theta_{i,t} \right), \quad (20)$$

where the sin/cosine transfer function is obviously exotic according to [16]. Defining a mean by the time-discrete weighted sum of MAP elements

$$\theta_{is,t+1} = \sum_{k=0}^{Z-1} \omega_{ik} \theta_{k,t+1} = \frac{Z}{M} \theta_{t+1}, \quad (21)$$

we can assume a relatively cooled state, where all elements could synchronize to a common precession dynamics with dynamic coupling

strength $\omega_{ik} = M^{-1}$ supporting eq.(10). The global mean represented by $\theta_{is,t+1}$ now behaves like a single MAP element in eq.(13) with charge Z and $j = JZ$

$$\theta_{is,t+1} = \frac{\pi J_i}{M} \sum_{k=0}^{Z-1} \cos(\theta_{ks,t}) = \pi \frac{J_i Z}{M} \cos(\theta_{is,t}). \quad (22)$$

This requires some symmetry conditions in precession dynamics, which can be achieved by a pair wise cancellation of cosine terms in the sum of eq.(22) with precession pairs $\cos\theta_1 + \cos\theta_2 = 0$ or by a symmetric distribution of local MAP angles around the mean $\theta_{is,t}$.

Since $SU(2)$ is the spin double cover of the group $SO(3)$, MAP could be relevant to relativistic quantum systems like the spin-orbit Eigenstates of a relativistic electron and also to “charged” spin network systems in the solid or nuclear range [3]. Free fall precession in curved space (with Berry-Hannay connection) can generate at the center a magnetic monopole if the blue point in fig.1 is a charge [9]. Magnetic monopoles are field configurations that arise naturally in gauge field theories, even at the classical level. A monopole requires the non-integrability of the phase of the wave function leading to a singularity. In MAP these are the singularities, where the nonlinear cosine equals the linear extra-precession term (see figs.3-5). With $j = JZ$, charge Z , spin J , and MJ the Dirac monopole charge quantum number, MAP type III could be related to the nature of the electromagnetic field and the vector potential. $M=137$, $J=0.5$, $Z=2$ (Cooper pairs) could be relevant to superconductivity with Berry’s phase part of the fine structure in the Josephson effect. The first bifurcation for a closed loop spin-network system (heavy nuclear particle) would occur near $Z=115.05275\dots$, see figs.3,5. Strong monopoles could be generated by MAP superconductor discs [3],[4].

4. Conclusions

It was found that a time-discrete chaotic system given by the cosine map can model a special recurrent holonomy with spin currents controlled and driven by precession, where the precession angle θ of a rotating rotor is proportional to the product of dynamical and geometric phase induced by precession. This follows naturally from eq.(7) if we assume that ψ , Δ , and the geometric phase evolve in time proportional to the precession frequency leading to the MAP condition $\theta NM = j\Delta$. Here the winding number j is the number of extra or missing rotor loops converted by holonomy into precession during a total cycle with N loops. The correspondent spin current is proportional to magnetic monopole charge M (acting like a von Klitzing conductivity or inverse magnetoresistance) and the gauge potential from the Berry connection (with MAP proportional to θ) indicating some relationship to low-temperature electromagnetism. The system shows bifurcation singularities in theory, experiments, and simulation, see computer experiments, the Powerball device [6], and Chua’s circuit approach [12]. One MAP element carries the symmetry of the Lorentz group $SO(3)$, near the holonomy attractor degrees of freedom get frozen to $SO(2)$ or $U(1)$. The geometric phase shows a

$2d$ to $1d$ mapping, where quantum-relativistic type II precession angles with space-time bending effects could generate closed loop periodicity conditions are supported by the Tschebyscheff polynomials. With synergetic effects given by a neural-type recursive network based on coupled MAP elements, a strong long range spin-network synchronization dynamics should be possible. In low-dimensional low-temperature systems the spin-currents of the Quantum Hall effect (where geometric phases play an important role [17]) could also be affected by a recurrent holonomy. Here it could be proper to synchronize the local $3d$ rotated rotations to a macroscopic $2d$ web-topology with dynamics approached by a recurrent rotation-translation model [18].

References

- [1] J. E. Marsden, T. Ratiu, Introduction to Mechanics and Symmetry, *Texts in Applied Mathematics* vol. 17, Springer-Verlag, 1994.
- [2] H. K. Chen, Chaos and Chaos Synchronization, *J. Sound Vib.* 255(4): 719-740, 2002.
- [3] B. Binder, "Geometric Phase Locked in Fine Structure" in *Iterative Coupling and Balancing Currents*, e-Book, ISBN:3-00-010972-2, 2003; "Berry's Phase and Fine Structure", <http://philsci-archive.pitt.edu/archive/00000682/>, updated at www.quanics.com/alfa137MN6.pdf, 2002, accessed 01.09.2002.
- [4] B. Binder, Magic Angle Precession, *AIP Conf. Proc.* 969: 1103-1110, 2008.
- [5] B. Binder, Magic Angle Precession at STAIF 2008, *Quanics Presentation notes*, www.quanics.com/MAPTalk20080214.pdf, 2008, accessed 14.02.2008.
- [6] L.A. Mishler, Gyroscopic Device, *United States Patent* 3,726,146, 1973.
- [7] P.G. Heyda, Roller ball dynamics Revisited, *Am. J. Phys.* 70: 1049-51, 2002.
- [8] W. F. Osgood, On the Gyroscope, *Transactions of the American Mathematical Society*, 23(3): 240-264, 1922.
- [9] W. F. Osgood, *Mechanics*, MacMillan, New York, 1937.
- [10] F. Wilczek, A. Zee, Appearance of Gauge Structure in Simple Dynamical Systems, *Phys. Rev. Lett.* 52: 2111, 1984.
- [11] A. Ishlinskii, Mechanics of Special Gyroscopic Systems, *Izd. AN USSR*, Kiev, 1952.
- [12] T. Matsumoto, L.O. Chua, M. Kumoro, The Double Scroll., *IEEE Transaction on Circuits and Systems*; CAS-32(8): 798-818, 1985.
- [13] C. Misner, K. Thorne, J. Wheeler, *Gravitation*, Freeman, 1973.
- [14] B. Binder, www.quanics.com/MAP_TableProcesses.pdf, accessed 12.03.2008.
- [15] B. Binder, Friedmann Propulsion in an Flat Holographic Universe, *AIP Conf. Proc.* 969: 1146-1153, 2008.
- [16] W. Duch, N. Jankowski, Transfer Functions: Hidden Possibilities for Better Neural Networks, 9th European Symposium on Artificial Neural Networks, 81-94, 2001.
- [17] K. S. Novoselov et. al, Unconventional quantum Hall effect and Berry's phase of 2π in bilayer graphene, *Nature Physics* 2, 177 - 180 (2006).
- [18] C.H. Skiadas, Ch. Skiadas, Chaos in Simple Rotation-Translation Models, arXiv:nlin/0701012v1 [nlin.CD] (2007).